

Ferromerrillite, $\text{Ca}_9\text{NaFe}^{2+}(\text{PO}_4)_7$, a new mineral from the Martian meteorites, and some insights into merrillite–tuite transformation in shergottites

SERGEY N. BRITVIN^{1,*}, SERGEY V. KRIVOVICHEV¹ and THOMAS ARMBRUSTER²

¹ Department of Crystallography, Institute of Geosciences, St. Petersburg State University, Universitetskaya Nab. 7/9, 199034 St. Petersburg, Russia

*Corresponding author, e-mail: sergei.britvin@spbu.ru

² Mineralogical Crystallography, Institute of Geological Sciences, University of Bern, Freiestrasse 3, 3012 Bern, Switzerland

Abstract: Ferromerrillite, ideally $\text{Ca}_9\text{NaFe}^{2+}(\text{PO}_4)_7$, is a new mineral related to the whitlockite group. It occurs as a common accessory phase in several Martian meteorites classified as basaltic and olivine-phyric shergottites. The mineral described herein originates from the two meteorites Shergotty (the type occurrence) and Los Angeles. Ferromerrillite is trigonal, space group $R\bar{3}c$; the unit-cell dimensions (single-crystal data) for material from Shergotty and Los Angeles are, respectively: a 10.372(2) and 10.3794(6); c 37.217(13) and 37.129(2) Å; V 3467(3) and 3464.1(1) Å³; $Z = 6$. The calculated density $D_{\text{calc.}}$ is 3.11 g/cm³ based on the empirical formula $\text{Ca}_{9.00}(\text{Na}_{0.60}\text{Ca}_{0.07})_{\Sigma 0.67}(\text{Fe}^{2+}_{0.53}\text{Mg}_{0.40})_{\Sigma 0.93}\text{P}_{7.08}\text{O}_{28}$ (Shergotty) and 3.14 g/cm³ for $\text{Ca}_{9.00}(\text{Na}_{0.49}\text{Ca}_{0.15})_{\Sigma 0.64}(\text{Fe}^{2+}_{0.78}\text{Mg}_{0.23})_{\Sigma 1.02}\text{P}_{7.03}\text{O}_{28}$ (Los Angeles). The crystal structure of ferromerrillite from the Los Angeles meteorite was solved and refined to $R_1 = 0.066$ on the basis of 1518 independent reflections with $I > 2\sigma(I)$. Single-crystal studies reveal that ferromerrillite grains from the two studied shergottites are heavily deformed with an angular mosaicity reaching 7 degrees. The latter imply that the mineral grains experienced a shock event but the impact pressure was not high enough (<23 GPa) for the transformation to tuite, $\gamma\text{-Ca}_3(\text{PO}_4)_2$, to occur. Ferromerrillite is colourless, no cleavage was observed, Mohs' hardness is ~5. In the immersion liquids, the mineral is colourless and non-pleochroic. It is optically negative, uniaxial to anomalously biaxial with $2V$ up to $(-)$ 20°. Refractive indices are: ω 1.623(1) and 1.624(1), ε 1.621(1) and 1.621(1) for Shergotty and Los Angeles material, respectively. The mineral is named as Fe-dominant analogue of merrillite.

Key-words: ferromerrillite; merrillite; tuite; whitlockite; new mineral; crystal structure; calcium sodium iron phosphate; impact pressure; meteorite; shergottite; Mars.

Introduction

Recent studies of whitlockite-group minerals have widely extended our knowledge on the crystal chemistry of that family of phosphates. Besides the pre-IMA species whitlockite $\text{Ca}_9\text{Mg}(\text{PO}_3\text{OH})(\text{PO}_4)_6$ (Fron del, 1941; Calvo & Gopal, 1975) and merrillite $\text{Ca}_9\text{NaMg}(\text{PO}_4)_7$ (Wherry, 1917; Hughes *et al.*, 2006, 2008; Jolliff *et al.*, 2006), the group now includes strontio whitlockite $\text{Sr}_9\text{Mg}(\text{PO}_3\text{OH})(\text{PO}_4)_6$ (Britvin *et al.*, 1991), bobdownsite $\text{Ca}_9\text{Mg}(\text{PO}_4)_6(\text{PO}_3\text{F})$ (Tait *et al.*, 2011), and wopmayite $\text{Ca}_6\text{Na}_3\text{Mn}(\text{PO}_4)_3(\text{PO}_3\text{OH})_4$ (Cooper *et al.*, 2013). The relationships between merrillite and whitlockite have been the subject of discussions for a long time (Gopal & Calvo, 1972; Prewitt & Rothbard, 1975; Dowty, 1977; Jolliff *et al.*, 2006; and the above cited references), with the emphasis on the role of sodium and hydrogen in their crystal structures. Water-containing minerals of the group (whitlockite itself,

strontio whitlockite, bobdownsite and wopmayite) are rare constituents of terrestrial hydrothermal associations; whitlockite is known as a common constituent of bone tissue (*e.g.* Jang *et al.*, 2014). Merrillite is a major accessory phosphate in meteorites and Lunar rocks (Wherry, 1917; Fuchs, 1969; Hughes *et al.*, 2006, 2008; Jolliff *et al.*, 2006) but virtually unknown in the Earth's rocks. The only reported terrestrial occurrence of merrillite is the locality in southeastern Siberia, Russia, where the mineral was found in mantle xenoliths and misidentified as whitlockite (Ionov *et al.*, 2006). The obvious gap between the ubiquity of merrillite in extraterrestrial rocks and its nearly complete lack on the Earth can be related to the absence of water and fluorine in the corresponding rock-forming systems: merrillite occurs in anhydrous, high-temperature and fluorine-poor environments (Fuchs, 1969; Hughes *et al.*, 2006; 2008; Ionov *et al.*, 2006; Jolliff *et al.*, 2006). Among the extraterrestrial occurrences of merrillite, there is a

small but cosmochemically important group of stony meteorites known as shergottites, named after the witnessed meteorite fall at Shergotty (now Sherghati), Bihar, India, in 1865 (Stöffler *et al.*, 1986; Grady, 2000). It is accepted that shergottites are the meteorites of Martian origin (Stolper & McSween, 1979; Papike, 1998); hence their study substantially contributes to the understanding of Martian mineralogy, petrology and geochemistry, complementary to the direct Mars exploration provided by the Mars rover missions (Economou, 2001; Christensen *et al.*, 2004; Rieder *et al.*, 2004; Clark *et al.*, 2005; McSween *et al.*, 2006; Schmidt *et al.*, 2009; Usui *et al.*,

2009; Bish *et al.*, 2013; Poulet *et al.*, 2014; Sautter *et al.*, 2014). Merrillite is an accessory phase in shergottites; in the basaltic and olivine-phyric (Goodrich, 2002) subgroups of those meteorites, the mineral is substantially enriched in iron, which substitutes for magnesium. Moreover, several basaltic and olivine-phyric shergottites, including Shergotty itself (Table 1), contain the Fe^{2+} -dominant analogue of merrillite which is considered, according to the current IMA nomenclature, as a new mineral species. We have studied that mineral from two basaltic shergottites: Shergotty (the type occurrence) and Los Angeles (Warren *et al.*, 2004). The mineral is named ferromerrillite as the

Table 1. Chemical composition of ferromerrillite from shergottite meteorites.

Meteorite	No. of points	Na ₂ O	K ₂ O	CaO	MgO	MnO	FeO	SiO ₂	P ₂ O ₅	Total	Notes
Shergotty	8	1.7		46.8	1.5		3.5		46.2	99.7	
	1	1.42	0.08	45.7	1.48	0.10	4.33	0.08	46.1	99.29	1
	2	1.3	0.1	47.1	1.5	0.1	4.2	0.1	44.7	99.1	
	1	1.27		46.2	1.44	0.16	4.21	0.12	44.4	97.8	
	9	1.5		47.7	1.3		4.0		45.1	99.6	
Los Angeles	10	1.4		47.0	0.9		5.2		45.7	100.2	
	1	0.67	0.04	44.16	0.75	0.19	4.69	0.1	45.59	96.19	2
	2	1.2		46.9	0.91		4.96	0.11	44.9	98.97	
QUE 94201	2	1.12		46.55	0.87	0.00	4.74	0.12	45.05	98.45	3
	2	0.3		44.1	0.6	0.2	5.5	0.1	45.9	96.7	4
	2	0.45		43.85	0.45	0.25	5.9	0.1	45.9	96.9	
NWA 480	1	0.54	0.01	47.3	0.61	0.25	6.1	0.08	44.58	99.47	5
	1	0.66		47.73	0.84	0.11	5.2	0.1	45.4	100.04	6
EETA 79001	1	0.89	0.05	48.03	1.2	0.19	5.43	0.22	43.87	99.88	7
	1	0.64		46.8	0.87	0.29	5.42		46.6	100.62	8
KG 002	1	0.72		46.2	1.25		4.97	0.1	45.6	98.84	9
	17	1.25	0.07	47.1	1.00	0.10	4.8		45.3	99.76	10
Tissint	1	0.69		47.31	1.72		4.31	0.08	46.14	100.24	

	Formula amounts based on 28 oxygen atoms per formula unit									Reference
	Na	K	Ca	Mg	Mn	Fe	Si	P		
Shergotty	0.60	0.00	9.08	0.40	0.00	0.53	0.00	7.08	1	
	0.50	0.02	8.90	0.40	0.02	0.66	0.01	7.09	2	
	0.45	0.02	9.27	0.41	0.02	0.65	0.02	6.95	3	
	0.46	0.00	9.19	0.40	0.03	0.65	0.02	6.98	4	
	0.53	0.00	9.33	0.36	0.00	0.61	0.00	6.98	5	
Los Angeles	0.49	0.00	9.15	0.23	0.00	0.78	0.00	7.03	1	
	0.24	0.01	8.84	0.21	0.03	0.73	0.02	7.21	6	
	0.43	0.00	9.25	0.25	0.00	0.76	0.02	7.00	7	
QUE 94201	0.40	0.00	9.20	0.24	0.00	0.73	0.02	7.04	8	
	0.11	0.00	8.79	0.17	0.03	0.86	0.02	7.23	9	
	0.16	0.00	8.74	0.12	0.04	0.92	0.02	7.23	10	
NWA 480	0.19	0.00	9.34	0.17	0.04	0.94	0.01	6.95	11	
	0.23	0.00	9.31	0.23	0.02	0.79	0.02	7.00	12	
EETA 79001	0.32	0.01	9.47	0.33	0.03	0.84	0.04	6.84	3	
	0.22	0.00	9.03	0.23	0.04	0.82	0.00	7.11	7	
	0.26	0.00	9.06	0.34	0.00	0.76	0.02	7.07	13	
KG 002	0.44	0.01	9.23	0.27	0.00	0.73	0.00	7.02	14	
Tissint	0.24	0.00	9.15	0.46	0.00	0.65	0.01	7.05	15	

Notes: [1] Al_2O_3 0.30; [2] $\text{V}_2\text{O}_5 + \text{Al}_2\text{O}_3 + \text{TiO}_2$ 0.06; [3] Y_2O_3 0.16; [4] Al_2O_3 0.1; [5] $\text{NiO} + \text{Al}_2\text{O}_3 + \text{TiO}_2$ 0.07; [6] $\text{NiO} + \text{TiO}_2$ 0.05; Al_2O_3 0.08; [8] Al_2O_3 0.05; [9] $\text{Ce}_2\text{O}_3 + \text{Y}_2\text{O}_3$ 0.25, SrO 0.02; [10] Ce_2O_3 0.10.

References: [1] This work; [2] Stolper & McSween, 1979; [3] Neville, 1987; [4] Lundberg *et al.*, 1988; [5] Sano *et al.*, 2000; [6] Mikouchi, 2001; [7] Greenwood *et al.*, 2003; [8] Warren *et al.*, 2004; [9] Mikouchi *et al.*, 1996; [10] Mikouchi *et al.*, 1998; [11] Kring *et al.*, 2003; [12] Barrat *et al.*, 2002; [13] Wang *et al.*, 2004; [14] Llorka *et al.*, 2013; [15] Balta *et al.*, 2015.

Fe^{2+} -dominant analogue of merrillite. Both the mineral and its name have been approved by the Commission on New Minerals, Nomenclature and Classification (CNMNC) of the International Mineralogical Association (IMA 2006–039). The holotype specimen of ferromerrillite from Shergotty is deposited in the Fersman Mineralogical Museum, Russian Academy of Sciences, Moscow, catalogue # 3514/1.

Occurrence and physical properties

Merrillite-group minerals having a composition consistent with that of ferromerrillite were previously reported from several basaltic and olivine-phyric shergottites (Table 1), where they occur as accessory phases associated with clinopyroxene and maskelynite (the impact-melted plagioclase glass). Due to the scarcity of the rock material from Shergotty (~50 mg) and Los Angeles (~200 mg) available in our hands, we were unable to prepare thin sections from those meteorites; their petrology, however, is thoroughly described in the literature (Stolper & McSween, 1979; Stöffler *et al.*, 1986; Mikouchi, 2001; Greenwood *et al.*, 2003; Warren *et al.*, 2004). Ferromerrillite grains from our shergottite samples have been pre-concentrated, after gentle grinding, using the sink-float method in heavy liquids ($\text{CHBr}_3\text{-CH}_2\text{I}_2\text{-ethanol}$). The obtained mineral concentrates have been further inspected in an immersion liquid ($n = 1.625$) from which ferromerrillite grains have been hand-separated under polarizing microscope. In total, we have extracted about 20 anhedral grains (15–20 μm in size) of ferromerrillite from the sample of Shergotty and about 30 grains (20–50 μm) from the sample of Los Angeles. Ferromerrillite grains are colourless and have no observable cleavage. They are non-fluorescent under short- and long-wave ultraviolet light. Lustre is vitreous. Mohs' hardness of the mineral is about 5. In the immersion liquids, ferromerrillite is

colourless and non-pleochroic. It is optically negative, uniaxial to anomalously biaxial with $2V$ up to $(-)\text{20}^\circ$. Refractive indices are: ω 1.623(1) and 1.624(1); ϵ 1.621(1) and 1.621(1) for the mineral from Shergotty and Los Angeles, respectively. The density of the mineral from Shergotty could not be measured due to the scarcity of the material and the danger of its loss; the calculated density is 3.11 g/cm^3 . The density of ferromerrillite from Los Angeles was measured by the sink-float method and found to be 3.14 g/cm^3 , in agreement with the calculated value of 3.17 g/cm^3 .

Chemical composition, structural studies and powder X-ray diffraction

A few grains of ferromerrillite from both shergottites were embedded into epoxy resin, gently polished, carbon coated and analyzed by means of an electron microprobe (CamScan 4 electron microscope equipped with Link AN1000 EDX analyzer, 20 kV, 1 nA), using the following analytical standards: chkalovite (Na), diopside (Mg), andradite (Fe), chlorapatite (Ca, P). The results are given in Table 1 along with the data previously reported in the literature. The chemical composition of the studied ferromerrillite from Shergotty corresponds to the empirical formula $\text{Ca}_{9.00}(\text{Na}_{0.60}\text{Ca}_{0.07})_{\Sigma 0.67}(\text{Fe}^{2+}_{0.53}\text{Mg}_{0.40})_{\Sigma 0.93}\text{P}_{7.08}\text{O}_{28}$ on the basis of 28 oxygen atoms per formula unit (*apfu*) whereas the average of analyses for Los Angeles ferromerrillite can be recalculated as $\text{Ca}_{9.00}(\text{Na}_{0.49}\text{Ca}_{0.15})_{\Sigma 0.64}(\text{Fe}^{2+}_{0.78}\text{Mg}_{0.23})_{\Sigma 1.02}\text{P}_{7.03}\text{O}_{28}$. These data are consistent with the previous reports on the mineral from Shergotty and Los Angeles (Table 1).

Preliminary single-crystal studies for ferromerrillite were performed by means of a Stoe IPDS II diffractometer (34-cm flat image plate detector), along with the single-crystal study of iron-free merrillite with the ideal formula $\text{Ca}_9\text{NaMg}(\text{PO}_4)_7$ (from the Brahin pallasite) for reference purposes. The reconstruction of reciprocal space for

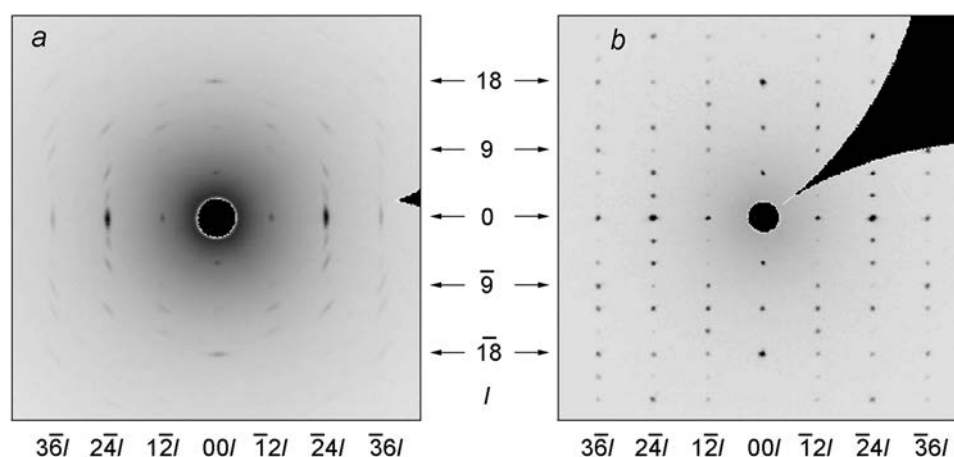


Fig. 1. Reconstruction of reciprocal space of (a) ferromerrillite (the Los Angeles meteorite) and (b) merrillite (the Brahin meteorite) along $[100]$, zero-layer.

Table 2. Crystal parameters, data collection and structure refinement details for ferromerrillite (Los Angeles shergottite) and merrillite (Brahin pallasite).

Mineral name	Ferromerrillite	Merrillite
Formula	$\text{Ca}_9(\text{Na}_{0.49}\text{Ca}_{0.19}\square_{0.32})(\text{Fe}^{2+}_{0.56}\text{Fe}^{3+}_{0.13}\text{Mg}_{0.31})(\text{PO}_4)_7$	$\text{Ca}_9\text{NaMg}(\text{PO}_4)_7$
Crystal size (mm)	$0.02 \times 0.02 \times 0.03$	$0.3 \times 0.3 \times 0.3$
Crystal system	Trigonal	Trigonal
Space group	$R3c$	$R3c$
a (Å)	10.3794(6)	10.3528(13)
c (Å)	37.129(2)	37.073(6)
V (Å ³)	3464.1(5)	3441.2(8)
Z	6	6
D_x (g/cm ³)	3.136	3.106
Instrument	Bruker Smart APEX DUO (CCD)	Stoe IPDS II (image plate)
Radiation	MoK α ($\lambda = 0.71073$ Å)	MoK α ($\lambda = 0.71073$ Å)
Average temperature (K)	293	293
θ range (degrees)	2.52–25.92	2.52–27.99
Total reflections	36895	9143
Unique reflections	1518	1866
Unique observed $ F_o \geq 4\sigma_F$	1420	1685
R_{int}	0.221	0.065
R_σ	0.047	0.042
Data completeness	1.000	1.000
$h;k;l$ range	–12,12; –12,12; –45,45	–13,13; –13,13; –48,48
R_1 ($ F_o \geq 4\sigma_F$)	0.066	0.031
R_1 (all data)	0.070	0.036
wR_2	0.180	0.068
$S = \text{Goof}$	1.128	0.992
Software	SHELX-97 (Sheldrick, 2008)	SHELX-97 (Sheldrick, 2008)

ferromerrillite from the Los Angeles shergottite revealed that the mineral grains are heavily deformed with an angular mosaicity reaching 7 degrees. The latter is illustrated by the comparison of reciprocal-space reconstructions for ferromerrillite and reference merrillite (Fig. 1). Due to

the small grain size and low quality of ferromerrillite from the Shergotty meteorite, we were unable to carry out its single-crystal studies, with the exception of the unit-cell parameters determination: trigonal, space group $R3c$, a 10.372(2), c 37.217(13), V 3467(3) Å³, $Z = 6$,

Table 3. Fractional atomic coordinates and displacement parameters in ferromerrillite from the Los Angeles shergottite.

Site	x	y	z	U_{11}	U_{22}	U_{33}	U_{23}	U_{13}	U_{12}	U_{iso}
Ca1	0.7268(3)	0.8581(3)	0.43127(6)	0.0289(12)	0.0295(12)	0.0339(10)	–0.0018(10)	–0.0002(10)	0.0157(10)	0.0303(6)
Ca2	0.6164(3)	0.8228(3)	0.23015(6)	0.0303(13)	0.0278(13)	0.0345(11)	–0.0010(12)	–0.0017(10)	0.0144(10)	0.0309(6)
Ca3	0.1245(3)	0.2706(3)	0.32427(7)	0.0310(13)	0.0402(14)	0.0406(11)	0.0066(11)	0.0007(11)	0.0194(11)	0.0366(6)
X^*	0	0	0.1864(3)	0.032(4)	0.032(4)	0.054(8)	0	0	0.016(2)	0.039(4)
M^{**}	0	0	–0.00078(11)	0.0241(13)	0.0241(13)	0.0342(18)	0	0	0.0121(6)	0.0275(11)
P1	0	0	0.26500(16)	0.0268(16)	0.0268(16)	0.046(3)	0	0	0.0134(8)	0.0333(11)
P2	0.6881(4)	0.8617(4)	0.13366(7)	0.0297(15)	0.0296(15)	0.0366(16)	0.0027(13)	0.0020(13)	0.0163(12)	0.0313(7)
P3	0.6563(4)	0.8485(3)	0.03004(8)	0.0246(14)	0.0285(15)	0.0360(14)	–0.0006(15)	–0.0010(12)	0.0137(13)	0.0295(6)
O1	0	0	0.3054(5)	0.016(4)	0.016(4)	0.067(10)	0	0	0.008(2)	0.033(3)
O2	0.0049(11)	0.8617(9)	0.2515(3)	0.031(4)	0.036(5)	0.061(5)	–0.011(4)	0.003(4)	0.018(4)	0.0419(19)
O3	0.7368(10)	0.9149(10)	0.1724(3)	0.033(4)	0.031(4)	0.055(5)	0.004(4)	0.002(4)	0.017(4)	0.0396(19)
O4	0.7597(10)	0.7733(10)	0.1196(2)	0.040(5)	0.032(5)	0.048(5)	0.012(4)	0.013(4)	0.020(4)	0.039(2)
O5	0.7235(9)	0.0008(9)	0.1111(2)	0.032(4)	0.031(4)	0.041(4)	0.002(3)	0.003(3)	0.018(4)	0.0336(18)
O6	0.5160(10)	0.7605(9)	0.1303(3)	0.030(5)	0.023(4)	0.055(5)	–0.004(3)	0.004(4)	0.014(4)	0.0362(19)
O7	0.6015(10)	0.9545(10)	0.0428(2)	0.037(5)	0.046(5)	0.044(4)	–0.003(4)	0.004(4)	0.030(4)	0.0379(19)
O8	0.5791(10)	0.7008(10)	0.0497(2)	0.040(5)	0.026(4)	0.046(4)	0.009(3)	0.004(4)	0.014(4)	0.039(2)
O9	0.8244(10)	0.9222(10)	0.0375(2)	0.023(4)	0.036(5)	0.042(4)	0.003(3)	0.000(3)	0.017(4)	0.0325(18)
O10	0.6227(10)	0.8203(9)	0.9901(2)	0.031(4)	0.026(4)	0.042(4)	–0.002(3)	–0.004(3)	0.014(3)	0.0332(18)

*Occupancy: ($\text{Na}_{0.49}\text{Ca}_{0.19}\square_{0.32}$) taking into account microprobe data. **Charge balanced occupancy: ($\text{Fe}^{2+}_{0.56}\text{Fe}^{3+}_{0.13}\text{Mg}_{0.31}$); e.s.d. of the refined Fe/Mg occupancies is 0.02.

Table 4. Fractional atomic coordinates and displacement parameters in the iron-free merrillite from the Brahin pallasite.

Site	x	y	z	U_{11}	U_{22}	U_{33}	U_{23}	U_{13}	U_{12}	U_{iso}
Ca1	0.72791(10)	0.85836(10)	0.43139(2)	0.0141(4)	0.0137(4)	0.0102(3)	-0.0013(3)	0.0000(3)	0.0072(3)	0.01254(17)
Ca2	0.61626(10)	0.82393(9)	0.23004(2)	0.0135(4)	0.0127(4)	0.0100(3)	-0.0001(4)	-0.0018(3)	0.0056(3)	0.01250(18)
Ca3	0.12359(9)	0.26904(10)	0.32388(2)	0.0148(4)	0.0209(4)	0.0128(4)	0.0020(3)	-0.0009(3)	0.0101(4)	0.01564(18)
X(Na)	0	0	0.18556(9)	0.0241(11)	0.0241(11)	0.0229(19)	0	0	0.0121(5)	0.0237(8)
M(Mg)	0	0	-0.00040(7)	0.0120(6)	0.0120(6)	0.0073(8)	0	0	0.0060(3)	0.0104(4)
P1	0	0	0.26517(5)	0.0117(5)	0.0117(5)	0.0122(7)	0	0	0.0059(2)	0.0119(3)
P2	0.68730(13)	0.86192(13)	0.13382(3)	0.0128(4)	0.0129(5)	0.0093(5)	0.0005(4)	0.0001(4)	0.0066(4)	0.0116(2)
P3	0.65600(13)	0.84931(12)	0.03004(3)	0.0114(4)	0.0123(5)	0.0073(4)	0.0015(4)	0.0005(4)	0.0057(4)	0.0105(2)
O1	0	0	0.30644(14)	0.0204(17)	0.0204(17)	0.011(2)	0	0	0.0102(9)	0.0172(11)
O2	0.0039(4)	0.8615(3)	0.25162(10)	0.0193(13)	0.0176(16)	0.0209(14)	-0.0004(13)	0.0049(12)	0.0095(14)	0.0192(6)
O3	0.7417(4)	0.9190(4)	0.17239(8)	0.0226(15)	0.0207(15)	0.0084(13)	-0.0017(11)	-0.0019(12)	0.0104(14)	0.0174(6)
O4	0.7575(4)	0.7730(4)	0.11985(8)	0.0190(15)	0.0252(17)	0.0121(14)	0.0007(12)	0.0016(12)	0.0139(14)	0.0175(7)
O5	0.7235(3)	0.0009(3)	0.11095(7)	0.0148(14)	0.0150(14)	0.0102(12)	-0.0016(11)	-0.0013(11)	0.0055(12)	0.0142(6)
O6	0.5140(3)	0.7598(3)	0.13157(8)	0.0139(14)	0.0131(14)	0.0124(13)	0.0013(12)	0.0025(10)	0.0064(13)	0.0133(6)
O7	0.6039(3)	0.9573(3)	0.04230(7)	0.0150(14)	0.0223(15)	0.0090(13)	-0.0012(13)	-0.0008(11)	0.0099(12)	0.0152(6)
O8	0.5792(4)	0.7000(4)	0.05026(8)	0.0194(15)	0.0188(16)	0.0125(13)	0.0025(12)	-0.0001(13)	0.0054(13)	0.0187(6)
O9	0.8251(3)	0.9231(3)	0.03680(8)	0.0120(13)	0.0148(15)	0.0116(13)	-0.0015(12)	0.0000(11)	0.0067(13)	0.0128(6)
O10	0.6220(3)	0.8187(3)	0.98981(8)	0.0160(14)	0.0187(14)	0.0094(13)	-0.0006(12)	-0.0016(11)	0.0072(12)	0.0153(6)

$D_{\text{calc.}} = 3.11 \text{ g/cm}^3$ based on the empirical formula given above. The quality of the crystals of ferromerrillite from the Los Angeles meteorite and merrillite from the Brahin meteorite allowed solution and refinement of their crystal structures. The details of data collection are provided in Table 2; the atomic coordinates and selected interatomic bond distances are given in Tables 3–5. The high value of R_{int} (0.2212) is explained by the extremely high angular mosaicity of the crystal owing to impact shock experienced by the host meteorite and, consequently, by the mineral grains. That phenomenon is inherently typical for impact-shocked crystals from shergottite meteorites (*e.g.*, Dera *et al.*, 2002). At the same time, the high symmetry of the mineral (and hence, high multiplicity of the observed reflections) resulted in successful intensity averaging of the merged reflections and, consequently, in the good final R_1 value.

X-ray powder diffraction data were obtained for ferromerrillite from the two studied shergottites (Table 6). The theoretical powder pattern for ferromerrillite from the Los Angeles meteorite was calculated using Atoms v.6.1 software. Refinements of the unit-cell parameters based on the powder diffraction data gave the following results (for Shergotty and Los Angeles, respectively): a 10.370(9) and 10.379(2) Å; c 37.17(9) and 37.06(2) Å; V 3462(15) and 3457(3) Å³.

Oxidation state of iron in ferromerrillite

Ferromerrillite is an iron-dominant analogue of merrillite, hence the oxidation state of iron in the mineral can be of particular interest. It is generally accepted that the total iron contained in the meteoritic phosphates is in the ferrous state (references in Table 1), but in the case of shergottite meteorites and their phosphates this postulate might not be completely true. Indeed, the oxygen fugacities derived on the basis of shergottite compositions are higher than those determined for other meteorite groups (Herd, 2008), hence partial substitution of Fe^{3+} for Fe^{2+} in the shergottitic phosphates cannot be ruled out. Direct determination of Fe(II)/Fe(III) ratio on micrometre-scale objects is still a challenging task (*e.g.* Dyar *et al.*, 2014), therefore in this work we follow a crystal-chemical approach based on the bond-valence concept and statistical analysis of the lattice parameters of whitlockite-type phosphates.

The Mg-Fe substitution in the structure of merrillite occurs at the octahedral M site (Tables 3–5; Fig. 2). As the synthetic compound $\text{Ca}_9\text{NaFe}^{2+}(\text{PO}_4)_7$ – the end-member of the merrillite–ferromerrillite series – does exist (Lazoryak & Belik, 2000), there are no structural limitations for the existence of a continuous solid solution $\text{Ca}_9\text{NaMg}(\text{PO}_4)_7$ – $\text{Ca}_9\text{NaFe}^{2+}(\text{PO}_4)_7$

Table 5. Selected interatomic distances (Å) in ferromerrillite (Los Angeles) and merrillite (Brahin).

Bond	Distance		Bond	Distance	
	Ferromerrillite	Merrillite		Ferromerrillite	Merrillite
	Los Angeles	Brahin		Los Angeles	Brahin
Ca1-O2	2.451(10)	2.449(4)	X-O2 × 3	2.825(14)	2.848(5)
Ca1-O4	2.858(10)	2.837(4)	X-O3 × 3	2.470(9)	2.418(3)
Ca1-O5	2.482(8)	2.479(3)			
Ca1-O6	2.469(8)	2.476(3)	M-O6 × 3	2.107(10)	2.069(3)
Ca1-O6	2.487(9)	2.492(3)	M-O9 × 3	2.127(9)	2.091(3)
Ca1-O7	2.453(8)	2.477(3)			
Ca1-O8	2.338(9)	2.313(3)	P1-O1	1.501(19)	1.530(6)
Ca1-O10	2.377(9)	2.365(3)	P1-O2 × 3	1.545(8)	1.538(3)
Ca2-O2	2.365(9)	2.368(3)	P2-O3	1.533(10)	1.542(3)
Ca2-O3	2.425(10)	2.438(3)	P2-O4	1.532(9)	1.521(3)
Ca2-O4	2.440(9)	2.451(3)	P2-O5	1.545(8)	1.546(3)
Ca2-O5	2.374(8)	2.375(3)	P2-O6	1.560(9)	1.564(3)
Ca2-O7	2.649(9)	2.634(3)			
Ca2-O8	2.717(9)	2.688(3)	P3-O7	1.544(8)	1.533(3)
Ca2-O9	2.420(9)	2.423(3)	P3-O8	1.515(9)	1.534(3)
Ca2-O9	2.437(8)	2.438(3)	P3-O9	1.540(9)	1.541(3)
			P3-O10	1.517(9)	1.529(3)
Ca3-O1 × 3	2.533(6)	2.4998(17)			
Ca3-O2	3.043(11)	3.020(4)			
Ca3-O3	2.648(9)	2.630(3)			
Ca3-O4	2.522(9)	2.522(3)			
Ca3-O5	2.420(8)	2.415(3)			
Ca3-O7	2.387(9)	2.389(3)			
Ca3-O8	2.616(9)	2.633(3)			
Ca3-O10	2.501(8)	2.472(3)			
Ca3-O10	2.546(8)	2.541(3)			

Table 6. X-ray powder diffraction data for ferromerrillite from the Los Angeles and Shergotty meteorites.

Los Angeles*				Shergotty*				Los Angeles				Shergotty			
$I_{\text{obs.}}$	$d_{\text{obs.}}$	$I_{\text{calc.}}$	$d_{\text{calc.}}$	$I_{\text{obs.}}$	$d_{\text{obs.}}$	$d_{\text{calc.}}$	hkl	$I_{\text{obs.}}$	$d_{\text{obs.}}$	$I_{\text{calc.}}$	$d_{\text{calc.}}$	$I_{\text{obs.}}$	$d_{\text{obs.}}$	$d_{\text{calc.}}$	hkl
18	8.090	20	8.087	2	8.13	8.089	102	7	1.986	4	1.987			1.989	2.2.12
33	6.460	32	6.451	2	6.42	6.462	104			1	1.961				410
9	6.167	6	6.177			6.203	006	6	1.935	2	1.937				413
20	5.196	12	5.190	1	5.24	5.186	110	16	1.921	19	1.922	2	1.917	1.923	4.0.10
2	4.789	1	4.785				113	12	1.880	10	1.884	2	1.885	1.884	328
9	4.372	3	4.368			4.366	202	12	1.870	11	1.869	2	1.868	1.869	416
3	4.119	2	4.118				108			1	1.815				3.1.14
13	4.047	15	4.044	1	4.06	4.045	204	8	1.815	2	1.815	1	1.824	1.822	1.0.20
3	3.968	3	3.973				116	14	1.801	3	1.802	1	1.807	1.803	3.2.10
20	3.423	16	3.426	1	3.43	3.438	1.0.10	14	1.787	3	1.789	1	1.784	1.788	502
5	3.384	3	3.383			3.381	211			4	1.771			1.771	419
11	3.343	5	3.342			3.340	212	9	1.765	7	1.765			1.764	504
		1	3.226			3.233	208								2.3.11
		3	3.226				119			3	1.729	1	1.724	1.729	330
81	3.191	59	3.190	6	3.19	3.189	214	21	1.710	20	1.713	2	1.715	1.719	2.0.20
14	2.994	9	2.996	2	2.990	2.994	300			2	1.697			1.700	3.1.16
100	2.861	100	2.859	10	2.860	2.866	2.0.10	11	1.699	5	1.697	1	1.704	1.701	3.0.18
21	2.741	22	2.740	2	2.747	2.742	218			1	1.692				2.1.19
9	2.696	7	2.696	1	2.702	2.696	306	7	1.678	4	1.676	1	1.672	1.676	508
7	2.655	7	2.654			2.662	1.1.12	7	1.672	2	1.671				424
73	2.594	65	2.595	5	2.594	2.593	220	6	1.664	1	1.666				336
13	2.539	5	2.539			2.538	223	5	1.657	3	1.656				4.1.12
		2	2.539	1	2.544	2.549	1.0.14	4	1.625	3	1.627				3.2.14
13	2.498	7	2.504			2.508	2.1.10			1	1.622			1.629	2.1.20
5	2.487	3	2.487			2.486	311	3	1.616	1	1.617				5.0.10
		1	2.407				314			2	1.613				4.0.16
14	2.393	8	2.392				226	5	1.593	2	1.595				428
		1	2.392	1	2.394	2.392	2.1.11			2	1.593			1.595	339
5	2.361	4	2.363	1	2.357	2.362	315			2	1.590			1.590	514
		1	2.281				2.0.14	5	1.575	1	1.577				2.0.22
10	2.243	8	2.243			2.252	1.0.16								155
		1	2.231				402			1	1.544				517
		2	2.231				1.1.15	11	1.544	6	1.544	1	1.540	1.544	4.2.10
10	2.183	7	2.184				404			7	1.540			1.542	3.2.16
		1	2.184	1	2.175	2.183	2.1.13								4.1.15
9	2.151	10	2.151	1	2.153	2.154	3.0.12			3	1.525			1.524	518
3	2.085	3	2.088			2.093	2.1.14			1	1.509				3.3.12
10	2.062	5	2.069			2.070	3.1.10			2	1.509			1.514	2.1.22
		2	2.059				321	4	1.499	3	1.498			1.497	600
		2	2.059				2.0.16	3	1.481	1	1.480				5.1.10
		2	2.059				0.0.18								431
7	2.049	4	2.049			2.048	322	5	1.458	4	1.459	1	1.459	1.458	434
6	2.021	7	2.022	1	2.022	2.022	408								
		3	2.013			2.012	324								
		1	2.004				3.1.11								

* Los Angeles: Rigaku R-AXIS Rapid II diffractometer, curved image plate, Debye-Scherrer geometry, $D = 127.4$ mm, $\text{CoK}\alpha$, microfocus tube with rotating anode, mirror monochromator, 40 kV, 15 mA, exposure 30 min. Shergotty: Debye-Scherrer 57.3 mm diameter camera, $\text{FeK}\alpha$, Mn filter, 40 kV, 30 mA, exposure 8 h, visual estimation of the intensities.

(merrillite–ferromerrillite). However, the M site can be fully or partially occupied by trivalent cations, including Fe^{3+} (Table 7) (Lazoryak *et al.*, 1996; Deyneko *et al.*, 2014). In the latter case, the compensation of the acquired charge imbalance is achieved via vacancies in the X position (the sodium site in the ideal merrillite structure, see Tables 3–5, Fig. 2). The end-member of the latter series, $\text{Ca}_9\text{Fe}^{3+}(\text{PO}_4)_7$, does also exist (Lazoryak *et al.*, 1996; Table 7). In this respect, all the analyses of ferromerrillite

collected in Table 1 exhibit a significant deficit of Na; the lower extreme, in QUE 94201 shergottite, contains as low as 0.11 Na atom per formula unit (Mikouchi *et al.*, 1996). In that case, there can be two possible pathways for charge balance compensation: either partial oxidation of Fe^{2+} for Fe^{3+} , according to the substitution scheme $\text{NaFe}^{2+} \leftrightarrow \square\text{Fe}^{3+}$, or partial substitution of Na for Ca in the X position: $\text{NaFe}^{2+} \leftrightarrow \text{Ca}_{1/2}\square_{1/2}\text{Fe}^{2+}$. The possibility of the latter substitution scheme is structurally confirmed in

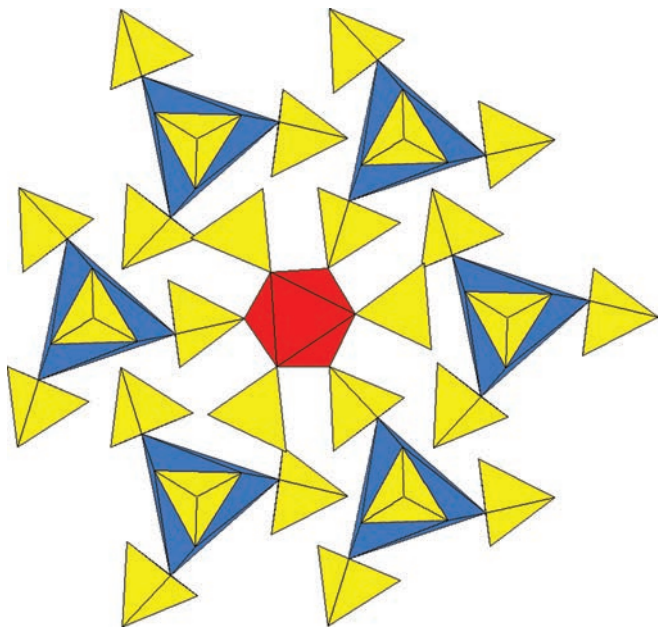


Fig. 2. Crystal structure of the ideal merrillite, $\text{Ca}_9\text{XM}(\text{PO}_4)_7$; projection onto (001). Red – (MO_6) octahedron; blue – (XO_6) polyhedron; yellow – (PO_4) tetrahedra. Calcium atoms have been omitted for clarity.

several natural and synthetic merrillites (Keil *et al.*, 1976; Dowty, 1977; Hughes *et al.*, 2008) and it allows keeping Fe in the divalent oxidation state. In order to ascertain that obvious ambiguity, we have carried out a simple statistical analysis based on the representative set of well characterized merrillite-type compounds (Table 7), excluding strontiowhitlockite (Britvin *et al.*, 1991) and REE-rich Lunar merrillite (Hughes *et al.*, 2006). It has been found that the a lattice parameter of the whitlockite-type compounds containing divalent cations correlates well with the mean atomic radius r of the M -site cation (Table 7, Fig. 3). The observed trend for M^{2+} -dominated whitlockites and merrillites (Fig. 3) can be well described by the equation:

$$a(\text{\AA}) = 9.840 + 0.70r \quad (R^2 = 0.83).$$

The two ferromerrillite samples studied in this work fit into the trend for the divalent cations, therefore one can assume that ferromerrillite from at least the Shergotty and Los Angeles meteorites does contain iron essentially in the divalent oxidation state. The calculations of bond-valence sums for the ferromerrillite and merrillite (Tables 8 and 9) corroborate the statistical data, confirming Fe^{2+} as the main form of iron in ferromerrillite. This result, along with the consistency of chemical compositions determined by electron microprobe (Table 1) and the freely refined M site occupancies in Los Angeles ferromerrillite (Table 3), proves that the studied mineral represents a new mineral species.

Ferromerrillite-tuite transformation: no evidence in Shergotty and Los Angeles

The occurrence of ferromerrillite in the Shergotty and Los Angeles meteorites raises several questions at the intercept of Martian basalts petrology, the origin of shergottites and the crystal chemistry of whitlockite-type phosphates. It is known that the majority of shergottite meteorites were subject to strong impact events. The first observed evidence for the high impact pressures experienced by shergottites was the transformation of plagioclase into maskelynite – the amorphous shock-induced calcium-sodium silicate glass (Stöffler, 1972; Stöffler *et al.*, 1986; Bischoff & Stöffler, 1992; Fritz *et al.*, 2005). Further studies revealed additional confirmations for ultra-high pressures experienced by several shergottites: the discovery of impact melt pockets containing ultra-dense silica polymorphs – stishovite, seifertite, and baddeleyite-type SiO_2 ; lingunite (hollandite-type $\text{NaAlSi}_3\text{O}_8$) (Gillet *et al.*, 2000), other unnamed dense silicate phases (El Goresy *et al.*, 2000, 2004, 2008, 2013) and tuite, $\gamma\text{-Ca}_3(\text{PO}_4)_2$. The latter mineral is of particular interest with respect to our study, because it is formed via the shock-induced transformation of merrillite (Xie *et al.*, 2002, 2003). Tuite, primarily discovered in the so-called “black impact veinlets” of shocked L6 chondrite Suizhou (Xie *et al.*, 2002, 2003) has later been reported in the basaltic shergottites Dar al Gani (DaG) 735 (Miyahara *et al.*, 2011) and North West Africa (NWA) 4468 (Boonsue & Spray, 2012). As shown in Fig. 1, the ferromerrillite grains studied in this work exhibit a high degree of angular mosaicity, suggesting that they experienced substantial mechanical (probably shock-induced) deformation (*e.g.* Bischoff & Stöffler, 1992). However, we could not identify tuite in the studied samples: X-ray powder diffraction data confirm only a merrillite-type phase (Table 6). According to Xie *et al.*, 2002; 2003), the transformation of merrillite into tuite requires shock pressures attaining 23 GPa. At the same time, recent studies of high-pressure mineral assemblages in shergottites raised substantial doubts on the claim that the peak impact pressures experienced by the majority of these meteorites could exceed 22 GPa (El Goresy *et al.*, 2013). In accordance with the results published in the latter work, our data on ferromerrillite from the Shergotty and Los Angeles meteorites show that these shergottites, though subjected to shock events, have never experienced impact pressures exceeding 22 GPa. In that respect, the structural confirmation of merrillite-type phosphates in shergottites can provide valuable information on the genesis of those meteorites.

Acknowledgements: The authors thank Sergey Vasiliev (SV-Meteorites, Prague) for providing the meteorite specimens. This research was financially supported by Russian Foundation for Basic Research grant no. 14-05-00910 and SPSU grant no. 3.38.136.2014. X-ray diffraction studies have been performed at the X-ray Diffraction Centre of St. Petersburg State University.

Table 7. Lattice parameters (\AA), M site occupancies, mean ionic radii r of the M -site cation (\AA) and occurrences of whitlockite-type phosphate minerals in comparison with the related synthetic compounds.

Name	Simplified formula	a	c	Mg	Fe ²⁺	Fe ³⁺	Mn ²⁺	Al	r	Occurrence/Synthesis	Ref.*
Merrillite	Ca ₉ NaMg(PO ₄) ₇	10.3528(13)	37.073(6)	1.00					0.720	Brahin meteorite	1
<i>Synthetic</i>	Ca ₉ NaMg(PO ₄) ₇	10.3397(1)	37.029(1)	1.00					0.720	Calcination	7
<i>Synthetic</i>	Ca ₉ NaMg(PO ₄) ₇	10.3405(2)	37.0736(8)	1.00					0.720	Calcination	12
<i>Synthetic</i>	Ca ₉ (Ca,□)Mg(PO ₄) ₇	10.3597(5)	37.161(4)	1.00					0.720	Hydrothermal/calcination	10
<i>Synthetic</i>	Ca ₉ (Ca,□)Mg(PO ₄) ₇	10.3499(2)	37.115(1)	1.00					0.720	Hydrothermal/calcination	10
Whitlockite	Ca ₉ Mg[PO ₃ (OH,F)](PO ₄) ₆	10.3477(2)	37.077(1)	1.00					0.720	Tip Top Mine, S. Dakota, U.S.A.	10
<i>Synthetic</i>	Ca ₉ Mg(PO ₃ OH)(PO ₄) ₆	10.350(5)	37.085(12)	1.00					0.720	Hydrothermal	2
<i>Synthetic</i>	Ca ₉ Mg(PO ₃ OH)(PO ₄) ₆	10.3571(2)	37.138(1)	1.00					0.720	Hydrothermal	10
Bobdownsite	Ca ₉ Mg(PO ₃ F)(PO ₄) ₆	10.3394(3)	37.084(2)	1.00					0.720	Tip Top Mine, S. Dakota, U.S.A.	11
Unnamed	Ca ₉ (Ca,□)(Mg,Fe)(PO ₄) ₇	10.362(1)	37.106(5)	0.78	0.22				0.733	Angra dos Reis meteorite	3
Bobdownsite	Ca ₉ Mg(PO ₃ F)(PO ₄) ₆	10.3224(3)	37.070(2)	0.72	0.04	0.13		0.11	0.694	Big Fish River, Yukon, Canada	11
Merrillite	(Ca,REE) ₉ (Na,□)Mg(PO ₄) ₇	10.2909(10)	36.8746(68)	0.71	0.31		0.01		0.739	Fra Mauro Formation, Moon	9
Whitlockite	Ca ₉ (Mg,Fe)(PO ₃ OH)(PO ₄) ₆	10.3590(3)	37.086(2)	0.62	0.35		0.02	0.02	0.739	Palermo, New Hampshire, U.S.A.	11
Whitlockite	Ca ₉ (Mg,Fe)(PO ₃ OH)(PO ₄) ₆	10.3612(6)	37.096(4)	0.60	0.32	0.07	0.09		0.746	Palermo, New Hampshire, U.S.A.	10
Ferromerrillite	Ca ₉ (Na,Ca)(Fe,Mg)(PO ₄) ₇	10.372(2)	37.217(13)	0.40	0.53				0.754	Shergotty meteorite	1
Ferromerrillite	Ca ₉ (Na,Ca)(Fe,Mg)(PO ₄) ₇	10.3794(6)	37.129(2)	0.23	0.78				0.766	Los Angeles meteorite	1
<i>Synthetic</i>	Ca ₉ NaFe(PO ₄) ₇	10.3703(3)	37.067(1)		1.00				0.780	Calcination/reduction	15
<i>Synthetic</i>	Ca ₉ Fe(PO ₃ OD)(PO ₄) ₇	10.36921(9)	37.1289(3)		1.00				0.780	Hydrothermal	8
<i>Synthetic</i>	Ca ₉ (Fe,Mg)H _{0.37} (PO ₄) ₇	10.3533(1)	37.1097(4)	0.37		0.63			0.676	Hydrothermal	14
<i>Synthetic</i>	Ca ₉ □Fe(PO ₄) ₇	10.3391(2)	37.130(1)			1.00			0.650	Calcination	6
Wopmayite	Ca ₆ Na ₃ □Mn(PO ₄) ₃ (PO ₃ OH) ₄	10.3926(2)	37.1694(9)	0.11	0.14	0.11	0.56	0.08	0.768	Tanco Mine, Manitoba, Canada	13
<i>Synthetic</i>	Ca ₉ Mn(PO ₃ OH)(PO ₄) ₇	10.438(2)	37.15(1)				1.00		0.830	Hydrothermal	4
Strontio-whitlockite	Str ₉ Mg(PO ₃ OH)(PO ₄) ₆	10.644(9)	39.54(6)	1.00					0.720	Kovdor Mine, Kola, Russia	5

*References: [1] This work; [2] Gopal *et al.*, 1974; [3] Keil *et al.*, 1976; Dowty, 1977; [4] Kostiner & Rea, 1976; [5] Britvin *et al.*, 1991; [6] Lazoryak *et al.*, 1996; [7] Morozov *et al.*, 1997; [8] Belik *et al.*, 2002; [9] Hughes *et al.*, 2006; [10] Hughes *et al.*, 2008; [11] Tait *et al.*, 2011; [12] Xia *et al.*, 2013; [13] Cooper *et al.*, 2014; [14] Deyneko *et al.*, 2014; [15] Lazoryak & Belik (PDF 51–0422).

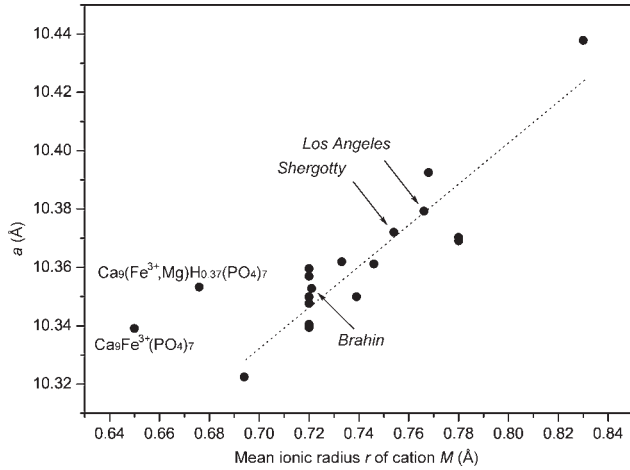


Fig. 3. Correlation between mean ionic radius of cation M and the a lattice parameter for the selected whitlockite-type compounds. The linear fit ($R^2 = 0.83$) for divalent cation-dominated structures is given as a dashed line.

References

- Balta, J.B., Sanborn, M.E., Udry, A., Wadhwa, M., Mcswen, H.Y. (2015): Petrology and trace element geochemistry of Tissint, the newest shergottite fall. *Meteor. Planet. Sci.*, **50**, 63–85.
- Barrat, J.A., Gillet, Ph., Sautter, V., Jambon, A., Javoy, M., Göpel, C., Lesourd, M., Keller, F., Petit, E. (2002): Petrology and chemistry of the basaltic shergottite North West Africa 480. *Meteor. Planet. Sci.*, **37**, 487–499.
- Belik, A.A., Izumi, F., Stefanovich, S. Yu., Lazoryak, B. I., Oikawa, K. (2002): Chemical and structural properties of a whitlockite-like phosphate, $\text{Ca}_9\text{FeD}(\text{PO}_4)_7$. *Chem. Mater.*, **14**, 3937–3945.
- Bischoff, A. & Stöffler, D. (1992): Shock metamorphism as a fundamental process in the evolution of planetary bodies; information from meteorites. *Eur. J. Mineral.*, **4**, 707–755.
- Bish, D.L., Blake, D.F., Vaniman, D.T., Chipera, S.J., Morris, R.V., Ming, D.W., Treiman, A.H., Sarrazin, P., Morrison, S.M., Downs, R.T., Achilles, C.N., Yen, A.S., Bristow, T.F., Crisp, J.A., Morookian, J.M., Farmer, J.D., Rampe, E.B., Stolper, E.M., Spanovich, N. (2013): X-ray diffraction results from mars science laboratory: Mineralogy of rocknest at Gale crater. *Science*, **341**, 1238932.

Table 8. Bond-valence (ν) calculations for ferromerrillite from the Los Angeles shergottite.

	M^{2+}	X	Ca1	Ca2	Ca3	P1	P2	P3	$\Sigma(\text{O})$
O1					0.22×3	1.37			2.03
O2		0.11×3	0.27	0.34	0.05	1.21×3			1.98
O3		0.27×3		0.29	0.16		1.25		1.97
O4			0.09	0.28	0.22		1.26		1.85
O5			0.25	0.33	0.29		1.21		2.08
O6	0.36×3		0.26				1.17		2.04
			0.25						
O7			0.27	0.16	0.32			1.22	1.97
O8			0.37	0.13	0.17			1.32	1.99
O9	0.33×3			0.29				1.23	2.14
				0.28					
O10			0.33		0.24			1.31	1.88
					0.21				
Σ	2.08	1.14	2.09	2.10	1.88	5.00	4.89	5.08	

Table 9. Bond-valence (ν) calculations for iron-free merrillite from the Brahmin pallasite.

	M	X	Ca1	Ca2	Ca3	P1	P2	P3	$\Sigma(\text{O})$
O1					0.24×3	1.27			1.99
O2		0.06×3	0.27	0.34	0.06	1.24×3			1.97
O3		0.19×3		0.28	0.17		1.22		1.86
O4			0.10	0.27	0.22		1.30		1.89
O5			0.25	0.33	0.30		1.21		2.09
O6	0.36×3		0.25				1.15		2.00
			0.24						
O7			0.25	0.16	0.32			1.25	1.98
O8			0.39	0.14	0.17			1.25	1.95
O9	0.34×3			0.29				1.23	2.14
				0.28					
O10			0.34		0.26			1.27	1.87
					0.21				
Σ	2.10	0.75	2.09	2.09	1.95	4.99	4.88	5.00	

- Boonsue, S. & Spray, J. (2012): Shock-induced phase transformations in melt pockets within Martian meteorite NWA 4468. *Spectroscopy Lett.*, **45**, 127–134.
- Britvin, S.N., Pakhomovskii, Ya. A., Bogdanova, A.N., Skiba, V.I. (1991): Strontio whitlockite, $\text{Sr}_9\text{Mg}(\text{PO}_3\text{OH})(\text{PO}_4)_6$, a new mineral species from the Kovdor deposit, Kola Peninsula, U.S.S.R. *Can. Mineral.*, **29**, 87–93.
- Calvo, C. & Gopal, R. (1975): The crystal structure of whitlockite from the Palermo Quarry. *Am. Mineral.*, **60**, 120–133.
- Christensen, P.R., Wyatt, M.B., Glotch, T.D., Rogers, A.D., Anwar, S., Arvidson, R.E., Bandfield, J.L., Blaney, D.L., Budney, C., Calvin, W.M., Fallacaro, A., Ferguson, R.L., Gorelick, N., Graff, T.G., Hamilton, V.E., Hayes, A.G., Johnson, J.R., Knudson, A.T., McSween, H.Y., Jr, Mehall, G.L., Mehall, L.K., Moersch, J.E., Morris, R.V., Smith, M.D., Squyres, S.W., Ruff, S.W., Wolff, M.J. (2004): Mineralogy at Meridiani Planum from the mini-TES experiment on the opportunity rover. *Science*, **306**, 1733–1739.
- Clark, B.C., Morris, R.V., McLennan, S.M., Gellert, R., Jolliff, B., Knoll, A.H., Squyres, S.W., Lowenstein, T.K., Ming, D.W., Tosca, N.J., Yen, A., Christensen, P.R., Gorevan, S., Brückner, J., Calvin, W., Dreibus, G., Farrand, W., Klingelhoefer, G., Waenke, H., Zipfel, J., Bell III, J.F., Grotzinger, J., McSween, H.Y., Rieder, R. (2005): Chemistry and mineralogy of outcrops at Meridiani Planum. *Earth Planet. Sci. Lett.*, **240**, 73–94.
- Cooper, M.A., Hawthorne, F.C., Abdu, Y. A., Ball, N.A. (2013): Wopmayite, ideally $\text{Ca}_6\text{Na}_3\text{Mn}(\text{PO}_4)_3(\text{PO}_3\text{OH})_4$, a new phosphate mineral from the Tanco Mine, Bernic Lake, Manitoba: description and crystal structure. *Can. Mineral.*, **51**, 93–106.
- Dera, P., Prewitt, C.T., Boctor, N.Z., Hemley, R.J. (2002): Characterization of a high-pressure phase of silica from the Martian meteorite Shergotty. *Am. Mineral.*, **87**, 1018–1023.
- Deyneko, D.V., Aksenov, S.M., Morozov, V.A., Stefanovich, S.Yu., Dimitrova, O.V., Barishnikova, O.V., Lazoryak, B.I. (2014): A new hydrogen-containing whitlockite type phosphate $\text{Ca}_9(\text{Fe}_{0.63}\text{Mg}_{0.37})\text{H}_{0.37}(\text{PO}_4)_7$: hydrothermal synthesis and structure. *Z. Kristallogr.*, **229**, 823–830.
- Dowty, E. (1977): Phosphate in Angra dos Reis: structure and composition of the $\text{Ca}_3(\text{PO}_4)_2$ minerals. *Earth Planet. Sci. Lett.*, **35**, 347–351.
- Dyar, M.D., Jawin, E.R., Breves, E., Marchand, G., Nelm, M., Lane, M.D., Mertzman, S.A., Bish, D.L., Bishop, J.L. (2014): Mössbauer parameters of iron in phosphate minerals: Implications for interpretation of martian data. *Am. Mineral.*, **99**, 914–942.
- Economou, T. (2001): Chemical analyses of martian soil and rocks obtained by the Pathfinder Alpha Proton X-ray spectrometer. *Rad. Phys. Chem.*, **61**, 191–197.
- El Goresy, A., Dubrovinsky, L.S., Sharp, T.G., Saxena, S.K., Chen, M. (2000): A monoclinic post-stishovite polymorph of silica in the Shergotty meteorite. *Science*, **288**, 1632–1634.
- El Goresy, A., Dubrovinsky, L.S., Sharp, T.G., Chen, M. (2004): Stishovite and post-stishovite polymorphs of silica in the Shergotty meteorite: their nature, petrographic settings versus theoretical predictions and relevance to Earth's mantle. *J. Phys. Chem. Solids*, **65**, 1597–1608.
- El Goresy, A., Dera, P., Sharp, T.G., Prewitt, C.T., Chen, M., Dubrovinsky, L.S., Wopenka, B., Boctor, N.Z., Hemley, R.J. (2008): Seifertite, a dense orthorhombic polymorph of silica from the Martian meteorites Shergotty and Zagami. *Eur. J. Mineral.*, **20**, 523–528.
- El Goresy, A., Gillet, Ph., Miyahara, M., Ohtani, E., Ozawa, S., Beck, P., Montagnac, G. (2013): Shock-induced deformation of Shergottites: shock-pressures and perturbations of magmatic ages on Mars. *Geochim. Cosmochim. Acta*, **101**, 233–262.
- Fritz, J., Greshake, A., Stöffler, D. (2005): Micro-Raman spectroscopy of plagioclase and maskelynite in Martian meteorites: evidence for progressive shock metamorphism. *Antarct. Meteor. Res.*, **18**, 96–116.
- Frondel, C. (1941): Whitlockite, a new calcium phosphate. *Am. Mineral.*, **26**, 145–152.
- Fuchs, L.H. (1969): The phosphate mineralogy of meteorites. *Astrophys. Space Sci. Library*, **12**, 683–695.
- Gillet, P., Chen, M., Dubrovinsky, L., El Goresy, A. (2000): Natural $\text{NaAlSi}_3\text{O}_8$ -hollandite in the shocked Sixiangkou meteorite. *Science*, **287**, 1633–1636.
- Goodrich, C.A. (2002): Olivine-phyric martian basalts: a new type of shergottite. *Meteor. Planet. Sci.*, **37**, B31–B34.
- Gopal, R. & Calvo, C. (1972): Structure relationship of whitlockite and $\beta\text{-Ca}_3(\text{PO}_4)_2$. *Nature Phys. Sci.*, **237**, 30–32.
- Gopal, R., Calvo, C., Ito, J., Sabine, W.K. (1974): Crystal structure of synthetic Mg-whitlockite, $\text{Ca}_{18}\text{Mg}_2\text{H}_2(\text{PO}_4)_4$. *Can. J. Chem.*, **52**, 1155–1164.
- Grady, M.M. (2000): Catalogue of meteorites (Fifth edition). The Natural History Museum, London. Cambridge University Press, Cambridge, UK, 689 p.
- Greenwood, J.P., Blake, R.E., Coath, C.D. (2003): Ion microprobe measurements of $^{18}\text{O}/^{16}\text{O}$ ratios of phosphate minerals in the Martian meteorites ALH84001 and Los Angeles. *Geochim. Cosmochim. Acta*, **67**, 2289–2298.
- Herd, C.D.K. (2008): Basalts as Probes of Planetary Interior Redox State. *Rev. Mineral. Geochem.*, **68**, 527–553.
- Hughes, J.M., Jolliff, B.L., Gunter, M.E. (2006): The atomic arrangement of merrillite from the Fra Mauro Formation, Apollo 14 lunar mission: The first structure of merrillite from the Moon. *Am. Mineral.*, **91**, 1547–1552.
- Hughes, J.M., Jolliff, B.L., Rakovan, J. (2008): The crystal chemistry of whitlockite and merrillite and the dehydrogenation of whitlockite to merrillite. *Am. Mineral.*, **93**, 1300–1305.
- Ionov, D.A., Hofmann, A.W., Merlet, C., Gurenko, A.A., Hellebrand, E., Montagnac, G., Gillet, P., Prikhodko, V.S. (2006): Discovery of whitlockite in mantle xenoliths: inferences for water- and halogen-poor fluids and trace element residence in the terrestrial upper mantle. *Earth Planet. Sci. Lett.*, **244**, 201–217.
- Jang, H.L., Jin, K., Lee, J., Kim, Y., Nahm, S.H., Hong, K.S., Nam, K.T. (2014): Revisiting whitlockite, the second most abundant biomineral in bone: nanocrystal synthesis in physiologically relevant conditions and biocompatibility evaluation. *ACS Nano*, **8**, 634–641.
- Jolliff, B.L., Hughes, J.M., Freeman, J.J., Zeigler, R.A. (2006): Crystal chemistry of lunar merrillite and comparison to other meteoritic and planetary suites of whitlockite and merrillite. *Am. Mineral.*, **91**, 1583–1595.
- Keil, K., Prinz, M., Hlava, P.F., Gomes, C.B., Curvello, W.S., Wasserburg, G.J., Tera, F., Papanastassiou, D.A., Huneke, J.C., Murali, A.V., Ma, M.-S., Schmitt, R.A., Lugmair, G.W., Marti, K., Scheinin, N.B., Clayton, R.N. (the ADORABLES) (1976): Progress by the consorts of Angra dos Reis. *Lunar Planet. Sci.*, **7**, 443–445.
- Kostiner, E. & Rea, J.R. (1976): The crystal structure of manganese-whitlockite, $\text{Ca}_{18}\text{Mn}_2\text{H}_2(\text{PO}_4)_{14}$. *Acta Cryst. B*, **32**, 250–253.
- Kring, D.A., Gleason, J.D., Swindle, T.D., Nishiizumi, K., Cafee, M.W., Hill, D.H., Jull, A.J.T., Boynton, W.V. (2003):

- Composition of the first bulk melt sample from a volcanic region of Mars: Queen Alexandra Range 94201. *Meteor. Planet. Sci.*, **38**, 1833–1848.
- Lazoryak, B.I. & Belik, A.A. (2000): Powder diffraction file, card 51–0422, ICDD.
- Lazoryak, B.I., Morozov, V.A., Belik, A.A., Khasanov, S.S., Shekhtman, V. Sh. (1996): Crystal structures and characterization of $\text{Ca}_9\text{Fe}(\text{PO}_4)_7$ and $\text{Ca}_9\text{FeH}_{0.9}(\text{PO}_4)_7$. *J. Solid State Chem.*, **122**, 15–21.
- Llorca, J., Roszjar, J., Cartwright, J.A., Bischoff, A., Ott, U., Pack, A., Merchel, S., Rugel, G., Fimiani, L., Ludwig, P., Casado, J.V., Allepuz, D. (2013): The Ksar Ghilane 002 shergottite - The 100th registered Martian meteorite fragment. *Meteor. Planet. Sci.*, **48**, 493–513.
- Lundberg, L.L., Crozaz, G., McKay, G., Zinner, E. (1988): Rare earth element carriers in the Shergotty meteorite and implications for its chronology. *Geochim. Cosmochim. Acta*, **52**, 2147–2163.
- McSween, H.Y., Wyatt, M.B., Gellert, R., Bell, J.F., Morris, R.V., Herkenhoff, K.E., Crumpler, L.S., Milam, K.A., Stockstill, K.R., Tornabene, L.L., Arvidson, R.E., Bartlett, P., Blaney, D., Cabrol, N.A., Christensen, P.R., Clark, B.C., Crisp, J.A., Des Marais, D.J., Economou, T., Farmer, J.D., Farrand, W., Ghosh, A., Golombek, M., Gorevan, S., Greeley, R., Hamilton, V.E., Johnson, J.R., Joliff, B.L., Klingelhöfer, G., Knudson, A.T., McLennan, S., Ming, D., Moersch, J.E., Rieder, R., Ruff, S.W., Schröder, C., de Souza, P.A., Squyres, S.W., Wänke, H., Wang, A., Yen, A., Zipfel, J. (2006): Characterization and petrologic interpretation of olivine-rich basalts at Gusev Crater, Mars. *J. Geophys. Res. E*, **111**, E02S10.
- Mikouchi, T. (2001): Mineralogical similarities and differences between the Los Angeles basaltic shergottite and the Asuka-881757 lunar mare meteorite. *Antarct. Meteorite Res.*, **14**, 1–20.
- Mikouchi, T., Miyamoto, M., McKay, G.A. (1996): Mineralogy and petrology of new Antarctic shergottite QUE94201: a coarse-grained basalt with unusual pyroxene zoning. *Lunar Planet. Sci.*, **27**, 879.
- , — (1998): Mineralogy of Antarctic basaltic shergottite Queen Alexandra Range 94201: similarities to Elephant Moraine A79001 (lithology B) martian meteorite. *Meteor. Planet. Sci.*, **33**, 181–189.
- Miyahara, M., Ohtani, E., Ozawa, S., Kimura, M., El Goresy, A., Sakai, T., Nagase, T., Hiraga, K., Hirao, N., Ohishi, Y. (2011): Natural dissociation of olivine to $(\text{Mg,Fe})\text{SiO}_3$ perovskite and magnesiowüstite in a shocked Martian meteorite. *Proc. Natl. Acad. Sci.*, **108**, 5999–6003.
- Morozov, V.A., Presnyakov, I.A., Belik, A.A., Khasanov, S.S., Lazoryak, B.I. (1997): Crystal structures of calcium magnesium alkali metal phosphates $\text{Ca}_9\text{MgM}(\text{PO}_4)_7$ ($\text{M} = \text{Li}, \text{Na}, \text{K}$). *Kristallogr. Rep.*, **42**, 758–769.
- Nevle, R.J. (1987): Phosphates in Shergotty and EETA79001: geochemistry and petrogenesis. *Lunar Planet. Sci.*, **18**, 714.
- Papike, J.J. (ed.) (1998): Planetary Materials. *Rev Mineral.*, **36**, Mineralogical Society of America, Washington, DC.
- Poulet, F., Carter, J., Bishop, J.L., Loizeau, D., Murchie, S.M. (2014): Mineral abundances at the final four Curiosity study sites and implications for their formation. *Icarus*, **231**, 65–76.
- Prewitt, C.T. & Rothbard, D.R. (1975): Crystal structures of meteoritic and lunar whitlockites. *Lunar Planet. Sci.*, **4**, 646–648.
- Rieder, R., Gellert, R., Anderson, R.C., Brückner, J., Clark, B.C., Dreibus, G., Economou, T., Klingelhöfer, G., Lugmair, G.W., Ming, D.W., Squyres, S.W., D’Uston, C., Wänke, H., Yen, A., Zipfel, J. (2004): Chemistry of rocks and soils at Meridiani Planum from the Alpha Particle X-ray Spectrometer. *Science*, **306**, 1746–1749.
- Sano, Y., Terada, K., Takeno, S., Taylor, L.A., McSween, H.Y., Jr. (2000): Ion microprobe uranium-thorium-lead dating of Shergotty phosphates. *Meteor. Planet. Sci.*, **35**, 341–346.
- Sautter, V., Fabre, C., Forni, O., Toplis, M.J., Cousin, A., Ollila, A.M., Meslin, P.Y., Maurice, S., Wiens, R.C., Baratoux, D., Mangold, N., Le Mouélic, S., Gasnault, O., Berger, G., Lasue, J., Anderson, R.A., Lewin, E., Schmidt, M., Dyar, D., Ehlmann, B.L., Bridges, J., Clark, B., Pinet, P. (2014): Igneous mineralogy at Bradbury Rise: The first Chemcam campaign at Gale Crater. *J. Geophys. Res. E*, **119**, 30–46.
- Schmidt, M.E., Farrand, W.H., Johnson, J.R., Schröder, C., Hurowitz, J.A., McCoy, T.J., Ruff, S.W., Arvidson, R.E., Des Marais, D.J., Lewis, K.W., Ming, D.W., Squyres, S.W., de Souza, P.A., Jr. (2009): Spectral, mineralogical, and geochemical variations across Home Plate, Gusev Crater, Mars indicate high and low temperature alteration. *Earth Planet. Sci. Lett.*, **281**, 258–266.
- Sheldrick, G.M. (2008): A short history of SHELX. *Acta Crystallogr. A*, **64**, 112–122.
- Stöffler, D. (1972): Deformation and transformation of rock-forming minerals by natural and experimental shock processes. I. Behavior of minerals under shock compression. *Fortschr. Mineral.*, **49**, 50–113.
- Stöffler, D., Ostertag, R., Jammes, C., Pfannschmidt, G., Sen Gupta, P.R., Simon, S.B., Papike, J.J., Beauchamp, R.H. (1986): Shock metamorphism and petrology of the Shergotty achondrite. *Geochim. Cosmochim. Acta*, **50**, 889–903.
- Stolper, E., McSween, H.Y., Jr. (1979): Petrology and origin of the shergottite meteorites. *Geochim. Cosmochim. Acta*, **43**, 1475–1498.
- Tait, K.T., Barkley, M.C., Thompson, R.M., Origlieri, M.J., Evans, S.H., Prewitt, C.T., Yang, H. (2011): Bobdownsite, a new mineral species from Big Fish River, Yukon, Canada, and its structural relationship with whitlockite-type compounds. *Can. Mineral.*, **49**, 1065–1078.
- Usui, T., McSween, H.Y., Jr., Clark III, B.C. (2009): Petrogenesis of high-phosphorous Wishstone Class rocks in Gusev Crater, Mars. *J. Geophys. Res. E*, **113**, E12S44.
- Wang, A., Kuebler, K.E., Jolliff, B.L., Haskin, L.A. (2004): Raman spectroscopy of Fe-Ti-Cr-oxides, case study: martian meteorite EETA79001. *Amer. Mineral.*, **89**, 665–680.
- Warren, P.H., Greenwood, J.P., Rubin, A.E. (2004): Los Angeles: a tale of two stones. *Meteor. Planet. Sci.*, **39**, 137–156.
- Wherry, E.T. (1917): Merrillite, meteoritic calcium phosphate. *Amer. Mineral.*, **2**, 119.
- Xia, Z., Liu, H., Li, X., Liua, C. (2013): Identification of the crystallographic sites of Eu^{2+} in $\text{Ca}_9\text{NaMg}(\text{PO}_4)_7$: structure and luminescence properties study. *Dalton Trans.*, **42**, 16588–16595.
- Xie, X., Minitti, M.E., Chen, M., Mao, H.-K., Wang, D., Shu, J., Fei, Y. (2002): Natural high-pressure polymorph of merrillite in the shock vein of the Suizhou meteorite. *Geochim. Cosmochim. Acta*, **66**, 2439–2444.
- Xie, X., Minitti, M.E., Chen, M., Mao, H.-K., Wang, D., Shu, J., Fei, Y. (2003): Tuite, $\gamma\text{-Ca}_3(\text{PO}_4)_2$: a new mineral from the Suizhou L6 chondrite. *Eur. J. Mineral.*, **15**, 1001–1005.

Received 31 May 2015

Modified version received 13 August 2015

Accepted 11 October 2015